A theory of inductive loops in electrochemical impedance spectroscopy

Yury Grabovsky* Jacob Guynee†

January 4, 2023

Abstract

We demonstrate that failure of time-invariance assumption in the modeling of electrochemical systems by equivalent circuits can lead to the formation of low frequency "inductive loops" that manifest themselves as positive imaginary parts of the impedance function. Assuming that the properties of the equivalent circuits change slowly in time we perform an asymptotic analysis and obtain a new integral representation of the impedance function that reduces to the standard one at high frequencies, while exhibiting inductive loops at low frequencies.

1 Introduction

Electrochemical impedance spectroscopy (EIS) is an indispensable tool to describe complex electrochemical systems in a unified and graphical way. In this approach any system is described by a single complex-valued impedance function $Z(\omega)$. The basic theory of EIS [19, 3, 4] says that this function possesses special analytic properties that are most concisely expressed by the representation

$$Z(\omega)=\frac{1}{iC_0\omega}+\int_0^\infty \frac{d\sigma(\tau)}{1+i\omega\tau},\qquad \int_0^\infty \frac{d\sigma(\tau)}{1+\tau}<+\infty,\quad 0<C_0\leq\infty. \tag{1}$$

Here σ is a positive Borel-regular measure on $[0,+\infty)$. It is often convenient to approximate such measures by linear combinations of delta-functions, resulting in rational approximations of $Z(\omega)$ [1]. Such approximations can be interpreted as impedances of electrical circuits made of resistors and capacitors only. They are called the equivalent circuit models (ECM). One easily verifiable feature of the representation (1) is the negativity of the imaginary part of the impedance function.

The experimentally observed arcs in a Nyquist plot of the impedance with positive imaginary part in the low frequency part of the spectrum received the unfortunate moniker of

*Department of Mathematics, Temple University, Philadelphia, PA 19122, USA.
†Department of Mathematics, Georgia Institute of Technology, Atlanta, GA 30332, USA.

an "inductive loop" [12, 8, 23, 21, 10]. It is generally agreed that magnetic effects play no significant role in the functioning of most electrochemical systems and devices, and even when they do, the inductive effects manifest themselves at the high end of the frequency spectrum [7, 16, 6]. The explanation of inductive loops in the current literature [16, 6] by means of ECMs with negative resistances and capacitances creates more problems than it solves. If one permits negative resistances and capacitances, then *arbitrary* "experimental data" can be matched by such an impedance function with any degree of precision due to the Riesz theorem (see e.g. [17, 14, 15]). This is not surprising, since it is the passivity of the system [22, 9, 20], violated by the the negative resistances and capacitances in ECMs, that are responsible for the possibility of stable reconstruction of the impedance function.

A far more reasonable explanation of the experimental appearance of low frequency inductive loops is the violation of the time-invariance assumption at time scales commensurate with the inverses of low frequencies. This explanation is semi-explicit in [21, 16, 18], where specific electrochemical processes altering the properties of the system on slow time scales are identified.

When the time-invariance assumption is violated the input-output behavior of the system can no longer be mathematically described by a well-defined impedance function at low frequencies. In this paper we will show that if one applies a particular impedance measurement procedure, delivering the correct impedance for any time-invariant system, the inductive loops could be observed in non time-invariant systems.

The goal of this paper is to extend the classical EIS/ECM approach to electrochemical systems with slowly "drifting" properties. In Section 3 we demonstrate that a single Voigt element with drifting properties may exhibit an inductive loop. In Section 4 we use asymptotic analysis to extend the EIS/ECM approach to non time-invariant systems with slowly varying properties. The resulting impedance representation formula, though more complicated, may still be used to reconstruct the impedance function values within the frequency band containing experimental measurements by performing the classical Kramers-Kronig analysis [2, 5, 11, 20] for high frequency data, while fitting the additional "drift" parameters using the inductive loop low frequency data.

The paper is organized as follows. In Section 2 we discuss a measurement technique that gives a good approximation of the true impedance function for time-invariant systems. We then show in Section 3 that the same measurement technique for non time-invariant Voigt elements can produce "inductive loop" data. Representing a general non time-invariant electrochemical system by an ECM with non time-invariant Voigt elements connected in series, gives us a mathematical model that can be analyzed. An asymptotic analysis applied to each non time-invariant Voigt element leads us in Section 4 to a generalization of the EIS theory that reduces to classical formulas at high frequencies and is capable of modeling low frequency inductive loops.

2 Impedance measurements

Let us assume that the input signal is the current

$$I(t) = I_0 \sin(\omega t), \quad t \in [0, T(\omega)], \quad T(\omega) = \frac{2\pi n(\omega)}{\omega}, \tag{2}$$

where $n(\omega) \in \mathbb{N}$ should be as large as possible, so that the time $T(\omega)$ it takes to make a measurement is still acceptable to whoever makes the measurements. Of course, this is an issue only for low frequencies ω. Thus, we can measure the system response only for frequencies $\omega \geq \omega_{\min} = 2\pi/T_{\max}$, where $T_{\max}$ is the maximal admissible time for making low frequency measurements. Hence, in the low frequency regime we always choose $n(\omega) = 1$. At high frequencies we use a different measurement strategy. We choose a fixed measurement time T_0 and set $n(\omega) =$`round`$(T_0\omega/2\pi)$. Hence, for all $\omega \geq \omega_{\min}$ we define

$$n(\omega) = \max\left\{1, \texttt{round}\left(\frac{T_0\omega}{2\pi}\right)\right\}, \qquad \omega \geq \omega_{\min}. \tag{3}$$

The Fourier transform of $I(t)$ can be computed explicitly, but is an unwieldy expression, except at the frequency ω of the input sinusoid:

$$\widehat{I}(\omega) = I_0 \int_0^{T(\omega)} \sin(\omega t) e^{-i\omega t} dt = \frac{\pi I_0 n}{i\omega} = \frac{I_0 T(\omega)}{2i}. \tag{4}$$

For linear, time-invariant (LTI) systems the output voltage $U(t)$ must satisfy $\widehat{U}(\omega) = Z(\omega)\widehat{I}(\omega)$, where the complex factor $Z(\omega)$ is called the impedance. Theoretically, when $I(t) = 0$ for $t > T(\omega)$, the output voltage is still non-zero. However, in most cases it decays exponentially fast and can therefore be neglected. In this case we have the approximation

$$\widehat{U}(\omega) \approx \int_0^{T(\omega)} U(t) e^{-i\omega t} dt. \tag{5}$$

Since $U(t)$ is measured, formula (5) can be used to estimate $\widehat{U}(\omega)$ and thus, we have the formula for estimating the impedance from the experimental data:

$$Z_0(\omega) = \frac{2i}{T(\omega)} \int_0^{T(\omega)} U(t) e^{-i\omega t} dt. \tag{6}$$

If we apply formula (6) to an elementary Voigt circuit, consisting of a resistor R and a capacitor C connected in parallel, we *will not* get the correct answer

$$Z_V(\omega) = \frac{R}{i\theta\omega + 1}, \qquad \theta = RC. \tag{7}$$

Figure 1 shows that Z_0 is not a very good approximation for Z_V, especially in the intermediate frequency range. The remedy is to understand this discrepancy and then devise a way to

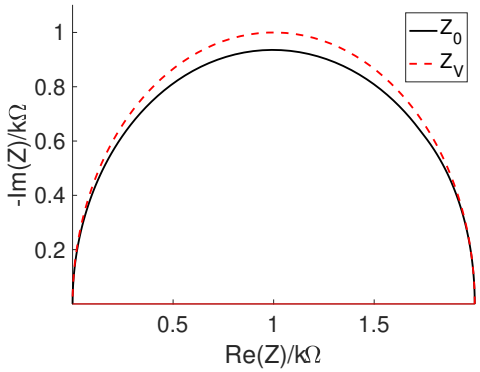

Figure 1: Comparison of $Z_0(\omega)$ and $Z(\omega)$ for an elementary Voigt circuit with $R = 2k\Omega$, $C = 200\mu F$.

correct for it. Using the explicit expression for $Z_0(\omega)$ (which we don't display here), we discover that for an elementary Voigt circuit we have

$$Z_0(\omega) = Z_V(\omega) - \left(\frac{1}{T\omega}\mathfrak{Im}(Z_V(\omega)) + \frac{i}{T}Z_V'(\omega)\right)\left(1 - e^{-\frac{T}{\theta}}\right), \tag{8}$$

where $Z_V'(\omega)$ denotes the derivative of $Z_V(\omega)$ with respect to ω. Since relation (8) between the measured and the true impedance function of an elementary Voigt circuit is linear, it extends to *all LTI systems*.

We recall that in an LTI system the output (voltage $U(t)$) depends on the input (current $I(t)$) via

$$U(t) = \rho_0 I(t) + \int_{-\infty}^{t} I(\tau)K(t-\tau)d\tau, \tag{9}$$

where the function $K(s)$ is called a memory kernel.

THEOREM **2.1.** *Suppose that the memory kernel decays exponentially:*

$$|K(s)| \leq \frac{R_0}{\theta}e^{-s/\theta}, \qquad s > T_0. \tag{10}$$

for some $T_0 < T(\omega)$ for all ω. Then

$$\left|Z_0(\omega) - Z(\omega) + \frac{1}{T\omega}\mathfrak{Im}(Z(\omega)) + \frac{i}{T}Z'(\omega)\right| \leq R_0\left(1 + \frac{\theta}{T}\right)e^{-T/\theta}, \tag{11}$$

where

$$Z(\omega) = \rho_0 + \int_0^{\infty} K(s)e^{-i\omega s}ds \tag{12}$$

is the true impedance of the system.

The proof can be found in Appendix A

Thus, we are lead to a simple method for estimating the true impedance by making measurements over a longer time $T_2 = 2\pi n_2(\omega)/\omega > T_1 = 2\pi n_1(\omega)/\omega$. Then, up to an exponentially small error we must have

$$Z(\omega) \approx Z_{\exp}(\omega) = \frac{T_2 Z_0(\omega; T_2) - T_1 Z_0(\omega; T_1)}{T_2 - T_1}. \tag{13}$$

We still want to require that at high frequencies the time it takes to make a an impedance measurement is fixed. Let us call it T_0', since we still want $n_1(\omega)$ to be given by (3). In that case

$$n_2^{\min}(\omega) = n_1(\omega) + 1 \leq n_2(\omega) \leq \max\left\{2, \texttt{round}\left(\frac{T_0'\omega}{2\pi}\right)\right\} = n_2^{\max}(\omega). \tag{14}$$

Thus, for measuring very low frequencies we set $n_1(\omega) = 1$ and $n_2(\omega) = 2$. When $\omega = 4\pi/T_0$ we have $n_1(\omega) = 2$, in which case we must require that $n_2(\omega) \geq 3$. It follows that $T_0' \geq 3T_0/2$, and therefore, $n_2^{\max}(\omega) > n_1(\omega)$. In practice, the experimenter can choose any integer $n_2(\omega)$ satisfying $n_2^{\min}(\omega) \leq n_2(\omega) \leq n_2^{\max}(\omega)$, once the constant $T_0' \geq 3T_0/2$ has been set.

The correction method (13) can be interpreted as a directive to ignore the transient response over the time interval $[0, T_1]$, effectively taking data during time interval $[T_1, T_2]$. Indeed, using formula (6), we have

$$Z_{\exp}(\omega) = \frac{2i}{T_2(\omega) - T_1(\omega)} \int_{T_1(\omega)}^{T_2(\omega)} U(t) e^{-i\omega t} dt, \qquad T_{1,2}(\omega) = \frac{2\pi n_{1,2}(\omega)}{\omega}. \tag{15}$$

One convenient choice is $n_1 = n(\omega)$ and $n_2 = 2n(\omega)$, where $n(\omega)$ is given by (3), so that the length of the time interval over which the data is taken is still $T(\omega) = 2\pi n(\omega)/\omega$.

THEOREM **2.2.** *Under assumptions of Theorem 2.1 we have the estimate*

$$|Z_{\exp}(\omega) - Z(\omega)| \leq \frac{T_1}{T_2 - T_1} R_0 \left(1 + \frac{\theta}{T_1}\right) e^{-T_1/\theta} + R_0 e^{-T_2/\theta}. \tag{16}$$

The proof can be found is in Appendix A.

To see how formula (15) improves the evaluation of the impedance we take the same Voigt circuit with $R = 2k\Omega$, $C = 200\mu F$, shown in Figure 1, and compare $Z_{\exp}(\omega)$ and $Z(\omega) = Z_V(\omega)$. The difference between the Nyquist plots of the two functions can no longer be visualized as in Figure 1, since it is less that 0.01%, according to numerics, when we choose $n_1 = n(\omega)$ and $n_2 = 2n(\omega)$.

3 Non time-invariant elementary Voigt circuits

In this section we examine elementary Voigt circuits made of a resistor and a capacitor connected in parallel. Our main assumption is that the parameters R and C of the circuit do not stay constant, but slowly change in time, instead. We will show that if we apply the impedance measurement recipe from the previous section to such non time-invariant systems we may obtain impedance curves with inductive loops.

3.1 General theory

Let us start by considering an elementary Voigt circuit consisting of a resistor $R = R(t)$ and a capacitor $C = C(t)$ connected in parallel. In such a circuit we have the Ohm's laws for each of the elements

$$I_R(t) = \frac{U(t)}{R(t)}, \qquad I_C(t) = C(t)\dot{U}(t).$$

Combining this with the Kirchhoff's law $I(t) = I_R(t) + I_C(t)$ we obtain the constitutive relation (i.e. dependence of $I(t)$ on $U(t)$) in the form

$$I(t) = \frac{U(t)}{R(t)} + C(t)\dot{U}(t). \tag{17}$$

Since we use the current as the input we need to solve (17) for $U(t)$:

$$U(t) = \int_{-\infty}^{t} \frac{I(s)}{C(s)} \exp\left\{-\int_s^t \frac{dx}{\theta(x)}\right\} ds, \qquad \theta = RC. \tag{18}$$

The quantity θ is called the relaxation time of the Voigt circuit. Formula (15) gives the experimentally measured "impedance" of a simple Voigt circuit with non time-invariant elements:

$$Z_{\exp}(\omega) = \frac{2i}{\Delta T}\int_{T_1}^{T_2} e^{-i\omega t}\int_0^t \frac{\sin(\omega s)}{C(s)} \exp\left\{-\int_s^t \frac{dx}{\theta(x)}\right\} dsdt, \quad \Delta T = T_2 - T_1. \tag{19}$$

For future reference we also have the following formula for the impedance of a non time-invariant capacitor and resistor

$$Z^C_{\exp}(\omega) = \frac{2i}{\Delta T}\int_{T_1}^{T_2} e^{-i\omega t}\int_0^t \frac{\sin(\omega s)}{C(s)} dsdt = \frac{2}{\Delta T\omega}\int_{T_1}^{T_2} (e^{-i\omega t} - 1)\frac{\sin(\omega t)}{C(t)} dt, \tag{20}$$

$$Z^R_{\exp}(\omega) = \frac{2i}{\Delta T}\int_{T_1}^{T_2} e^{-i\omega t} R(t)\sin(\omega t) dt. \tag{21}$$

3.2 Explicit non time-invariant models

Let us now examine a particular model of the time dependence of $R(t)$ and $C(t)$. We assume that R and C undergo an "exponential drift" from R_- (resp. C_-) at $t = -\infty$ to R_+ (resp. C_+) at $t = +\infty$:

$$R(t) = \frac{aR_- + R_+ e^{t/\tau}}{a + e^{t/\tau}}, \quad C(t) = \frac{bC_- + C_+ e^{t/\tau}}{b + e^{t/\tau}}, \quad a, b > 0. \tag{22}$$

The evolution law for $R(t)$ is governed by two parameters: the time scale τ and the "current position" $a > 0$ that tells us how far along $R(t)$ is on the way from R_- to R_+. It is in 1-1

correspondence with $R(0)$. The value $a = 1$ means $R(0)$ is exactly half-way between R_+ and R_-. Exact same comments apply to $C(t)$. It is easy to calculate explicitly

$$-\int_s^t \frac{dx}{\theta(x)} = \frac{\tau}{\theta_+}\left(\frac{s-t}{\tau} + \kappa_C \ln\left(\frac{\rho_C e^{-s/\tau}+1}{\rho_C e^{-t/\tau}+1}\right) + \kappa_R \ln\left(\frac{\rho_R e^{-s/\tau}+1}{\rho_R e^{-t/\tau}+1}\right)\right), \tag{23}$$

where

$$\kappa_C = \frac{(a-\rho_C)(b-\rho_C)}{\rho_C(\rho_C-\rho_R)}, \quad \kappa_R = \frac{(a-\rho_R)(b-\rho_R)}{\rho_R(\rho_R-\rho_C)}, \quad \rho_R = \frac{aR_-}{R_+}, \quad \rho_C = \frac{bC_-}{C_+}, \quad \rho_R \neq \rho_C.$$

We note a relation

$$\kappa_C + \kappa_R = 1 - \frac{\theta_+}{\theta_-}, \qquad \theta_\pm = C_\pm R_\pm. \tag{24}$$

If $\rho_R = \rho_C = \rho$, then

$$-\int_s^t \frac{dx}{\theta(x)} = \frac{\tau}{\theta_+}\left(\frac{s-t}{\tau} + \alpha \ln\left(\frac{\rho e^{-s/\tau}+1}{\rho e^{-t/\tau}+1}\right) + \frac{\beta(e^{-s/\tau}-e^{-t/\tau})}{(\rho e^{-s/\tau}+1)(\rho e^{-t/\tau}+1)}\right), \tag{25}$$

where

$$\alpha = 1 - \frac{\theta_+}{\theta_-}, \qquad \beta = \frac{(a-\rho)(b-\rho)}{\rho}.$$

A different drift model

$$R(t) = R_0 e^{-t/\tau} + R_\infty(1-e^{-t/\tau}), \qquad C(t) = C_0 e^{-t/\tau} + C_\infty(1-e^{-t/\tau}) \tag{26}$$

is a limiting case of our model (22) with $R_+ = R_\infty$, $C_+ = C_\infty$, and

$$a, b \to 0, \quad R_-, C_- \to \infty, \quad aR_- \to R_0 - R_\infty, \quad bC_- \to C_0 - C_\infty.$$

In this limit, however, the restriction that R_- and C_- are positive are no longer required, since $R(t)$ and $C(t)$ are required to be positive only for $t \geq 0$. In this drift model we can still use (23) with

$$\rho_R \to \frac{R_0}{R_\infty} - 1, \quad \rho_C \to \frac{C_0}{C_\infty} - 1, \quad \kappa_R \to \frac{\rho_R}{\rho_R - \rho_C}, \quad \kappa_C \to \frac{\rho_C}{\rho_C - \rho_R},$$

provided $\rho_R \neq \rho_C$. If $\rho_R = \rho_C = \rho$, then we use formula (25) with $\alpha = 1$ and $\beta = \rho$.

Once, $\int_s^t \theta(x)^{-1} dx$ has been evaluated, we compute

$$U(t) = \frac{I_0}{C_+}\int_0^t \sin(\omega s)\frac{1+be^{-s/\tau}}{\rho_C e^{-s/\tau}+1}\exp\left\{-\int_s^t \frac{dx}{\theta(x)}\right\} ds. \tag{27}$$

The experimenatally measured impedance $Z_{\exp}(\omega)$ is then computed by means of formula (15). The numerical evaluation of $Z_{\exp}(\omega)$ presents several challenges, since parameter τ must be very large, relaxation times $\theta_\pm$ are typically very small and ω can range from 10^{-6}Hz to 10^6Hz, making some integrands highly oscillatory. These issues are addressed in Appendix B. Figure 2 shows an inductive loop in the Nyquist impedance plot of a non time-invariant Voigt element, with $R(t)$ and $C(t)$ given by (22), where $R_+ = 0.4k\Omega$, $R_- = 2k\Omega$, $a = 10$, $C_+ = 1.6mF$, $C_- = 0.8mF$, $b = 6$, $\tau = 600s$. The figure shows that at high frequencies the impedance is very well captured by the impedance of the time-invariant Voigt element with $R = R(0)$, and $C = C(0)$.

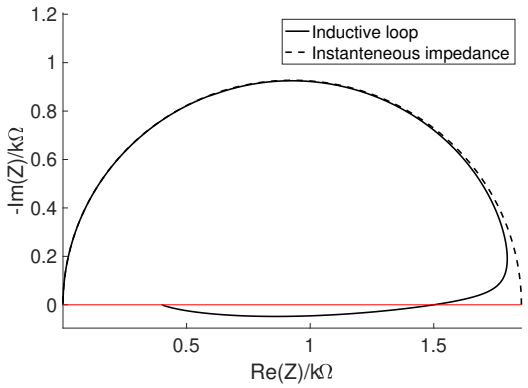

Figure 2: An inductive loop in a non time-invariant Voigt element.

4 Slow parameter drift asymptotics

Assume that $1/\tau = \epsilon$ is a small parameter and that $\omega = \epsilon\Omega$, where the rescaled frequency Ω is assumed to be fixed. We need to find the asymptotics of $Z(\epsilon\Omega)$ as $\epsilon \to 0$ and see if $\Im(Z(\epsilon\Omega))$ can indeed be positive. We now assume that $R(t) = R_0(\epsilon t)$ and $C(t) = C_0(\epsilon t)$, where $R_0(x)$ and $C_0(x)$ are strictly positive, bounded smooth functions with bounded first derivatives on $\mathbb{R}$. Our goal is not only to obtain the asymptotics of $Z(\omega)$, defined by (6), as $\epsilon \to 0$, but estimate the error between the actual impedance and its asymptotic approximation. We obtain for the elementary Voigt circuit, using (18)

$$Z_\epsilon(\omega) = \frac{2i}{\Delta T}\int_{T_1}^{T_2} e^{-i\omega t}\int_0^t \frac{\sin(\omega s)}{C_0(\epsilon s)}\exp\left\{-\int_s^t \frac{d\tau}{\theta(\epsilon\tau)}\right\} dsdt, \quad \Delta T = T_2 - T_1.$$

When the drift time scale $\tau = 1/\epsilon$ is large, the formula for $Z_\epsilon(\omega)$ above can be simplified:

$$Z_\epsilon(\omega) = \frac{i\Omega}{\pi\Delta n(\omega)}\int_{2\pi n_1(\omega)/\Omega}^{2\pi n_2(\omega)/\Omega} e^{-i\Omega\eta}\mathfrak{Im}\left(\frac{R_0(\eta)e^{i\Omega\eta}}{1+i\omega\theta_0(\eta)}\right) d\eta + O(\epsilon), \tag{28}$$

where the order ϵ error $O(\epsilon)$ is *uniform over the entire frequency spectrum.*

Formula (28) shows that if the functions $\theta_0(\eta)$ and $R_0(\eta)$ are constants, then the approximation becomes exact, as it reduces to the classical impedance of the elementary Voigt circuit. One more simplification is possible in the asymptotics $\epsilon \to 0$. Specifically, we can replace $\theta_0(\eta)$ by $\theta(0)$ in (28). Our final asymptotics is

$$Z^*_\epsilon(\omega) = Z(\omega,\Omega) = \frac{i\Omega}{\pi\Delta n(\omega)}\int_{2\pi n_1(\omega)/\Omega}^{2\pi n_2(\omega)/\Omega} e^{-i\Omega\eta}\mathfrak{Im}\left(\frac{R_0(\eta)e^{i\Omega\eta}}{1+i\omega\theta_0(0)}\right) d\eta. \tag{29}$$

For numerical evaluation of (29) we choose $n_1 = n(\omega)$, $n_2 = 2n(\omega)$ and change variables of integration $\eta = sn/\Omega$. Then, using the representation $\mathfrak{Im}(z) = (z-\overline{z})/2i$ we obtain the formula we use in the Matlab code to make Fig. 3:

$$Z^*_\varepsilon(\omega) = \frac{1}{2\pi}\int_{2\pi}^{4\pi}\frac{R_0\left(\frac{sn}{\Omega}\right)}{1+i\omega\theta_0(0)}ds - \frac{1}{2\pi}\int_{2\pi}^{4\pi}\frac{R_0\left(\frac{sn}{\Omega}\right)e^{-2ins}}{1-i\omega\theta_0(0)}ds. \tag{30}$$

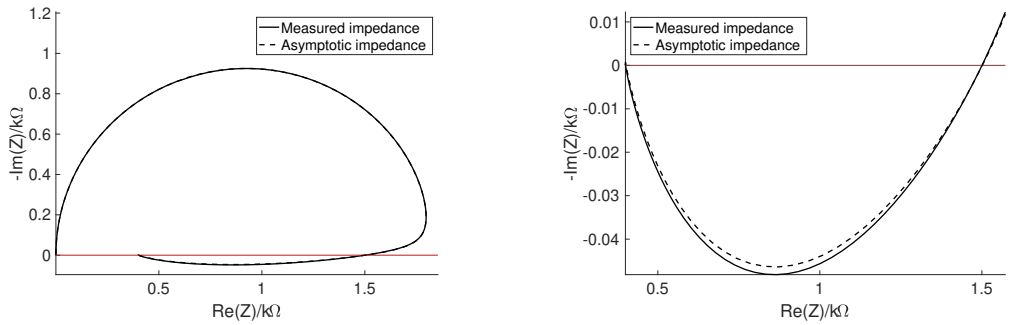

Figure 3: The quality of the asymptotics of an inductive loop.

For the model (22) we compute

$$\frac{1}{2\pi}\int_{2\pi}^{4\pi} R_0\left(\frac{sn}{\Omega}\right) ds = R_+ + \frac{(R_+ - R_-)\Omega}{2\pi n}\ln\left(1 + \frac{a(e^{-\frac{4\pi n}{\Omega}} - e^{-\frac{2\pi n}{\Omega}})}{1 + ae^{-\frac{2\pi n}{\Omega}}}\right).$$

In the high frequency regime

$$R_0\left(\frac{sn}{\Omega}\right) = R_0\left(\frac{\epsilon s T_0}{2\pi}\right)$$

We can therefore, use a linear approximation $R_0(x) \approx b_R + m_R x$, when $x \in [\epsilon T_0, 2\epsilon T_0]$, where the parameters b_R and m_R are found from the least squares fit. In that case

$$\frac{1}{2\pi}\int_{2\pi}^{4\pi} R_0\left(\frac{sn}{\Omega}\right) e^{-2ins} ds \approx \frac{im_R}{2\Omega}.$$

Figure 3 shows the Nyquist plot of $Z^*_\epsilon(\omega)$ superimposed on the computed "measured" impedance corresponding to the model (22). The difference between the two graphs is not detectable at the scale of the entire Nyquist plot, shown in the left panel of the figure. The right panel shows the blown-up portion of the plot containing the inductive loop. The overall relative error of the asymptotic approximation (29) is about 0.1%. In the figure we used (22) with the same parameter values as in Figure 2.

Now, if we have a general electrochemical system exhibiting parameter drift, then the measured impedance can be represented as

$$Z_{\rm exp}(\omega) = \frac{i\Omega}{\pi(n_2(\omega) - n_1(\omega))}\int_{2\pi n_1(\omega)/\Omega}^{2\pi n_2(\omega)/\Omega} e^{-i\Omega\eta}\mathfrak{Im}\left(Z(\omega,\eta)e^{i\Omega\eta}\right) d\eta + O(\epsilon), \tag{31}$$

where for each $\eta \in \mathbb{R}$ the function $\omega \mapsto Z(\omega,\eta)$ is a classical (instantaneous) impedance function, provided there is no leading capacitance in the ECM. In the presence of the leading capacitance, the term

$$Z^C_{\rm exp}(\omega) = \frac{i\Omega}{\pi(n_2(\omega) - n_2(\omega))}\int_{2\pi n_1(\omega)/\Omega}^{2\pi n_2(\omega)/\Omega} (e^{-i\Omega\eta} - 1)\frac{\sin(\Omega\eta)}{i\omega C_0(\eta)} d\eta$$

must be added to the right-hand side of (31).

If we approximate the instantaneous impedance function $Z(\omega, \epsilon t)$ by a finite Voigt circuit ECM [1]

$$Z(\omega, \eta) = R_0(\eta) + \sum_{j=1}^{N} \frac{R_j(\eta)}{1 + i\omega\theta(\eta)},$$

then, up to a uniform, over the entire spectrum, order ϵ error, we have

$$Z_{\exp}(\omega) = \frac{i\Omega}{\pi(n_2(\omega) - n_1(\omega))} \int_{2\pi n_1(\omega)/\Omega}^{2\pi n_2(\omega)/\Omega} e^{-i\Omega\eta} \mathfrak{Im}\left(Z^0(\omega, \eta) e^{i\Omega\eta}\right) d\eta + O(\epsilon), \tag{32}$$

where

$$Z^0(\omega, \eta) = R_0(\eta) + \sum_{j=1}^{N} \frac{R_j(\eta)}{1 + i\omega\theta(0)}. \tag{33}$$

If $R_j(\eta)$ in (33) are modeled according to (26),

$$R_j(\eta) = R_j(0) + \Delta R_j \left(1 - e^{-\mu_j \eta}\right), \quad j = 0, \ldots, N, \tag{34}$$

then the integral in (32) can be computed explicitly:

$$Z_{\exp}(\omega) = \sum_{j=0}^{N} \left\{ \frac{R_j(0) + \Delta R_j}{1 + i\omega\theta_j(0)} + \Delta R_j F\left(\frac{\epsilon\mu_j}{\omega}, \omega\theta_j(0)\right) \right\} + O(\epsilon), \tag{35}$$

where $\theta_0 = 0$, and

$$F(W, v) = i \frac{e^{-2\pi n_1 W} - e^{-2\pi n_2 W}}{\pi(n_2 - n_1)W} \frac{v(W + i) - 1}{(1 + v^2)(W + 2i)}.$$

Typically, one would choose $n_1(\omega) = n(\omega)$ and $n_2(\omega) = 2n(\omega)$, where $n(\omega)$ is given by (3). At low frequencies $n(\omega) = 1$, while at high frequencies $2\pi n(\omega)/\omega$ can be replaced with a constant T_0.

5 Conclusions and discussion

In this paper we have proposed an explanation of the inductive loop phenomena observed in experiments. The hypothesis is that the act of the impedance measurement of an electrochemical system might speed up slow processes, such as corrosion and charge diffusion, altering the properties of the system on time scales commensurate with the inverses of the frequencies at which the impedance is measured. The modeling and analysis of these processes can lead to specific drift laws that can be used to validate our general theory.

A natural question is whether our theory makes it apparent how the time-dependent nature of the system causes the occurrence of inductive loops. By way of the answer we refer to formula (30) and set $\omega = 0$, $n(\omega) = 1$. Then we obtain

$$\mathfrak{Im}(Z(\epsilon\Omega)) \approx \frac{1}{2\pi} \int_{2\pi}^{4\pi} R_0\left(\frac{s}{\Omega}\right) \sin(2s) ds \tag{36}$$

While $R_0(u)$ is a strictly positive, smooth real function, the sign of the integral in (36) is the outcome of balancing positive and negative contributions of the oscillatory integrand. For example, if $R_0(u)$ is a decreasing function, then positive contributions will always be larger than the negative ones and inductive loops will be present. Conversely, if $R_0(u)$ is an increasing function, no inductive loops will be produced. If the slowly oscillating sinusoidal current input causes a corresponding in-phase oscillation of R_0, the inductive loop effect could be several times stronger.

One open question, not directly addressed in the paper is capturing the time scale τ over which the system's properties change. A crude estimate would be the inverse frequency at which the imaginary part of the impedance hits zero. For example, in the simulation corresponding to Figure 2 the time scale $\tau = 600s$, while $2\pi/\omega_0 = 610s$, where $\mathfrak{Im}(Z(\omega_0)) = 0$. Our simulation of the time-dependent elementary Voigt circuit shows that the deviations from the classical model start at frequencies ω as large as two orders of magnitude over τ. They become vividly pronounced at frequencies on the order of $1/\tau$ and persist over frequencies an order of magnitude lower.

Finally, whether or not the inductive loop data can give additional information about the system beyond the time scale τ depends on whether the drift model (34) is acceptable. In this case one should be able to use the algorithm in [13] applied to the high frequency data to compute parameters $R_j(0)$, $\theta_j(0)$ and N. The intermediate and low frequency data can then be used in a non-linear least squares fit to to estimate drift parameters μ_j and ΔR_j. Future research into the inductive loops should address these questions.

Acknowledgments. This material is based upon work supported by the National Science Foundation under Grant No. DMS-2005538.

A Mathematical proofs

A.1 Proof of Theorem 2.1 and 2.2

For $I(t) = \chi_{[0,T(\omega)]}(t)\sin(\omega t)$ we have, making a change of variables $s = t - \tau$,

$$U(t) = \rho_0 \sin(\omega t) + \int_0^t K(s)\sin(\omega(t-s))ds, \qquad 0 \le t \le T(\omega).$$

We can then write

$$U(t) = \rho_0 \sin(\omega t) + \int_0^\infty \chi_{(s,+\infty)}(t)K(s)\sin(\omega(t-s))ds,$$

so that we can substitute this into (6) and switch the order of integration. We obtain

$$Z_0(\omega) = \rho_0 + \frac{2i}{T(\omega)}\int_0^{T(\omega)} K(s)\left(\int_s^{T(\omega)} \sin(\omega(t-s))e^{-i\omega t}dt\right)ds.$$

Computing the inner integral we obtain

$$Z_0(\omega) = \rho_0 + \int_0^{T(\omega)} K(s)\left(e^{-i\omega s} - \frac{\omega s e^{-i\omega s} - \sin(\omega s)}{2\pi n}\right)ds.$$

Using formula (12) for the true impedance, we compute

$$Z(\omega) - \frac{1}{2\pi n(\omega)}\mathfrak{Im}(Z(\omega)) - \frac{i\omega}{2\pi n(\omega)}Z'(\omega) = \rho_0 + \int_0^\infty K(s)\left(e^{-i\omega s} + \frac{\sin(\omega s) - \omega s e^{-i\omega s}}{2\pi n}\right) ds.$$

Therefore

$$Z(\omega) - \frac{\mathfrak{Im}(Z(\omega))}{\omega T(\omega)} - \frac{i}{T(\omega)}Z'(\omega) - Z_0(\omega) = \int_{T(\omega)}^\infty K(s)\left(e^{-i\omega s} + \frac{\sin(\omega s) - \omega s e^{-i\omega s}}{2\pi n}\right) ds. \quad (37)$$

For $s \geq T(\omega) = 2\pi n/\omega$ we have $\omega s \geq 2\pi n$. Denoting $x = \omega s$ and $A = 1/(2\pi n)$, we estimate

$$|e^{-ix} + A(\sin x - xe^{-ix})| \leq |1 - Ax| + A = Ax - 1 + A \leq Ax,$$

since $Ax \geq 1$ and $A \leq 1/(2\pi) < 1$. Hence,

$$\left| Z_0(\omega) - Z(\omega) + \frac{\mathfrak{Im}(Z(\omega)) + i\omega Z'(\omega)}{2\pi n(\omega)} \right| \leq \frac{1}{T(\omega)} \int_{T(\omega)}^\infty s|K(s)|ds.$$

Using the exponential decay (10) of the memory kernel we obtain the estimate

$$\left| Z_0(\omega) - Z(\omega) + \frac{\mathfrak{Im}(Z(\omega)) + i\omega Z'(\omega)}{2\pi n(\omega)} \right| \leq R_0\left(1 + \frac{\theta}{T(\omega)}\right) e^{-\frac{T(\omega)}{\theta}}, \quad (38)$$

proving (11).

Let us now prove Theorem 2.2. We compute,

$$Z_{\exp}(\omega) - Z(\omega) = \frac{T_1}{T_2 - T_1}\int_{T_1}^{T_2} K(s)\left(e^{-i\omega s} + \frac{\sin(\omega s) - \omega s e^{-i\omega s}}{2\pi n_1}\right) ds - \int_{T_2}^\infty K(s)e^{-i\omega s}ds.$$

Uisng estimate (38) we obtain

$$|Z_{\exp}(\omega) - Z(\omega)| \leq \frac{T_1(\omega)}{T_2(\omega) - T_1(\omega)} R_0\left(1 + \frac{\theta}{T_1(\omega)}\right) e^{-\frac{T_1(\omega)}{\theta}} + R_0 e^{-\frac{T_2(\omega)}{\theta}}.$$

A.2 Proof of the asymptotic foormula (31)

Let us analyze the asymptotic behavior of $Z_\epsilon(\omega)$. We first change variables in the innermost integral $\sigma = \epsilon\tau$:

$$Z_\epsilon(\omega) = \frac{2i}{\Delta T}\int_{T_1}^{T_2} e^{-i\omega t}\int_0^t \frac{\sin(\omega s)}{C_0(\epsilon s)} \exp\left\{-\frac{1}{\epsilon}\int_{\epsilon s}^{\epsilon t}\frac{d\sigma}{\theta(\sigma)}\right\} ds dt.$$

Next we change variables $\xi = \epsilon s$ in the integral with respect to the s variable:

$$Z_\epsilon(\omega) = \frac{2i}{\Delta T\epsilon}\int_{T_1}^{T_2} e^{-i\omega t}\int_0^{t\epsilon} \frac{\sin(\omega\xi/\epsilon)}{C_0(\xi)} \exp\left\{-\frac{1}{\epsilon}\int_{\xi}^{\epsilon t}\frac{d\sigma}{\theta(\sigma)}\right\} d\xi dt.$$

Finally, we change variables in the outermost integral $\eta = \epsilon t$:

$$Z_\epsilon(\omega) = \frac{2i}{\Delta T \epsilon^2} \int_{T_1\epsilon}^{T_2\epsilon} e^{-i\Omega\eta} \int_0^\eta \frac{\sin(\Omega\xi)}{C_0(\xi)} \exp\left\{-\frac{1}{\epsilon}\int_\xi^\eta \frac{d\sigma}{\theta(\sigma)}\right\} d\xi d\eta,$$

where $\Omega = \omega/\epsilon$ could be large, when ω is not very small, but could also be of order 1, when ω is of order ϵ.

The main approximation idea is to realize that

$$E_\epsilon(\xi,\eta) = \exp\left\{-\frac{1}{\epsilon}\int_\xi^\eta \frac{d\sigma}{\theta(\sigma)}\right\}$$

is exponentially small when $\eta - \xi$ is not very small. However, when $\eta \approx \xi$, then $\theta(\sigma) \approx \theta(\eta)$, which means that

$$E_\epsilon(\xi,\eta) \approx E_\epsilon^0(\xi,\eta) = \exp\left\{-\frac{\eta-\xi}{\theta(\eta)\epsilon}\right\}.$$

To make this approximation quantitative we use the inequality

$$\frac{e^{x_2} - e^{x_1}}{x_2 - x_1} < e^{\max\{x_1,x_2\}},$$

which is a consequence of convexity of the exponential function. Hence,

$$|E_\epsilon(\xi,\eta) - E_\epsilon^0(\xi,\eta)| \le \frac{L_{\theta^{-1}}(\eta-\xi)^2}{2\epsilon} \exp\left\{-\frac{\eta-\xi}{M_\theta\epsilon}\right\} = \epsilon L B\left(\frac{\eta-\xi}{\epsilon}\right),$$

where

$$M_\theta = \max_{t\in\mathbb{R}} \theta(t), \qquad L_{\theta^{-1}} = \max_{t\in\mathbb{R}} \left|\left(\frac{1}{\theta(t)}\right)'\right|, \qquad B(x) = \frac{x^2}{2}\exp\left\{-\frac{x}{M_\theta}\right\}.$$

Thus, we can replace $Z_\epsilon(\omega)$ with its approximation

$$Z_\epsilon^{(1)}(\omega) = \frac{2i}{\Delta T \epsilon^2} \int_{T_1\epsilon}^{T_2\epsilon} e^{-i\Omega\eta} \int_0^\eta \frac{\sin(\Omega\xi)}{C_0(\xi)} E_\epsilon^0(\xi,\eta) d\xi d\eta.$$

Moreover, we also have

$$|Z_\epsilon(\omega) - Z_\epsilon^{(1)}(\omega)| \le \frac{2L_{\theta^{-1}}}{m_C \Delta T \epsilon} \int_{T_1\epsilon}^{T_2\epsilon} \int_0^\eta B\left(\frac{\eta-\xi}{\epsilon}\right) d\xi d\eta,$$

where

$$m_C = \min_{t\in\mathbb{R}} C(t).$$

Changing variables in the inner integral $x = (\eta - \xi)/\epsilon$ we obtain

$$|Z_\epsilon(\omega) - Z_\epsilon^{(1)}(\omega)| \le \frac{2L_{\theta^{-1}}\epsilon}{m_C} \int_0^\infty B(x)dx = \frac{\epsilon M_\theta^3 L_{\theta^{-1}}}{m_C}.$$

The function $E_\epsilon^0(\xi,\eta)$ is exponentially small when ξ is not very close to η. However, when ξ is very close to η we can replace $C_0(\xi)$ with $C_0(\eta)$. Hence we have

$$Z_\epsilon^{(1)}(\omega) \approx Z_\epsilon^{(2)}(\omega) = \frac{2i}{\Delta T \epsilon^2} \int_{T_1\epsilon}^{T_2\epsilon} \frac{e^{-i\Omega\eta}}{C_0(\eta)} \int_0^\eta \sin(\Omega\xi) E_\epsilon^0(\xi,\eta) d\xi d\eta.$$

Moreover,

$$|Z_\epsilon^{(1)}(\omega) - Z_\epsilon^{(2)}(\omega)| \le \frac{2L_{C^{-1}}}{\Delta T \epsilon^2} \int_{T_1\epsilon}^{T_2\epsilon} \int_0^\eta (\eta-\xi) \exp\left\{-\frac{\eta-\xi}{\epsilon M_\theta}\right\} d\xi d\eta,$$

where

$$L_{C^{-1}} = \max_{t\in\mathbb{R}} \left| \left(\frac{1}{C(t)}\right)' \right|.$$

Changing variables $x = (\eta-\xi)/\epsilon$ in the inner integral we obtain the bound

$$|Z_\epsilon^{(1)}(\omega) - Z_\epsilon^{(2)}(\omega)| \le \frac{2L_{C^{-1}}}{\Delta T} \int_{T_1\epsilon}^{T_2\epsilon} \int_0^\infty x \exp\left\{-\frac{x}{M_\theta}\right\} dx d\eta = 2L_{C^{-1}} M_\theta^2 \epsilon.$$

Now, the inner integral in $Z_\epsilon^{(2)}(\omega)$ can be evaluated explicitly:

$$\int_0^\eta \sin(\Omega\xi) \exp\left\{-\frac{\eta-\xi}{\theta(\eta)\epsilon}\right\} d\xi = \frac{\epsilon\theta\sin(\Omega\eta) - \epsilon^2\theta^2\Omega\cos(\Omega\eta) + \epsilon^2\theta^2\Omega e^{-\eta/(\epsilon\theta)}}{1+\epsilon^2\theta^2\Omega^2}.$$

We observe that the first two terms can be combined nicely, and

$$Z_\epsilon^{(2)}(\omega) = \frac{2i}{\Delta T\epsilon} \int_{T_1\epsilon}^{T_2\epsilon} e^{-i\Omega\eta} \mathfrak{Im}\left(\frac{R_0(\eta)e^{i\Omega\eta}}{1+i\omega\theta_0(\eta)}\right) d\eta + \Delta_\epsilon(\omega) = Z_\epsilon^{(3)}(\omega) + \Delta_\epsilon(\omega),$$

where

$$\Delta_\epsilon(\omega) = \frac{2i\Omega}{\Delta T} \int_{T_1\epsilon}^{T_2\epsilon} e^{-i\Omega\eta} \frac{\theta^2 e^{-\eta/(\epsilon\theta)}}{C_0(\eta)(1+\epsilon^2\theta^2\Omega^2)} d\eta.$$

We estimate

$$|\Delta_\epsilon(\omega)| \le 2\Omega\epsilon \max_{\eta\in[T_1\epsilon,T_2\epsilon]} \frac{\theta(\eta)^2 e^{-\eta/\epsilon\theta(\eta)}}{C_0(\eta)(1+\epsilon^2\theta(\eta)^2\Omega^2)} \le M_R e^{-T_1/M_\theta}.$$

$Z_\epsilon^{(3)}(\omega)$ can be written as a two-scale impedance function (28).

In order to prove a simplified formula (29) we estimate

$$|Z_\epsilon^{(3)}(\omega) - Z_\epsilon^*(\omega)| \le \frac{\Omega}{\pi\Delta n(\omega)} \frac{M_R L_\theta}{1+m_\theta^2\omega^2} \int_{2\pi n_1(\omega)/\Omega}^{2\pi n_2(\omega)/\Omega} \omega\eta d\eta = \frac{2\pi\epsilon(n_1+n_2)M_R L_\theta}{1+m_\theta^2\omega^2}.$$

If we choose $n_1 = n$ and $n_2 = 2n$, then in the regime $n(\omega) = 1$ we get the bound

$$|Z_\epsilon^{(3)}(\omega) - Z_\epsilon^*(\omega)| \le 6\pi\epsilon M_R L_\theta.$$

If $n(\omega) > 1$, then $n(\omega) = T_0\omega/2\pi$, and we obtain

$$|Z_\epsilon^{(3)}(\omega) - Z_\epsilon^*(\omega)| \leq \frac{3\epsilon T_0 \omega M_R L_\theta}{1 + m_\theta^2 \omega^2} \leq \frac{3\epsilon T_0 M_R L_\theta}{2m_\theta}.$$

Hence, we obtain a uniform in the entire spectrum bound

$$|Z_\epsilon(\omega) - Z_\epsilon^*(\omega)| \leq M\epsilon$$

for some constant M that depends on the parameter functions $R_0(s)$ and $C_0(s)$, and that scales like $R\theta$.

B Numerical evaluation of the impedance in explicit drift models

The key to the effective numerical computation of $Z_{\exp}(\omega)$ for explicit drift models (22) and (26) is a non-dimensionalization of all quantities. We therefore begin by rescaling the variable of integration in the definition (19) of $Z(\omega)$, $t = n\hat{t}/\omega$.

$$Z(\omega) = \frac{i}{I_0\pi} \int_{2\pi}^{4\pi} U\left(\frac{n\hat{t}}{\omega}\right) e^{-in\hat{t}} d\hat{t},$$

where we have chosen $n_1 = n(\omega)$, $n_2 = 2n(\omega)$, and where $n(\omega)$ is given by (3). We then observe that $U(t)$ has the form

$$U(t) = \frac{I_0}{C_+} \int_0^t \sin(\omega s) f\left(\frac{s}{\tau}\right) e^{\frac{\tau}{\theta_+}\left[g\left(\frac{s}{\tau}\right) - g\left(\frac{t}{\tau}\right)\right]} ds, \tag{39}$$

where

$$f(u) = \frac{be^{-u} + 1}{\rho_C e^{-u} + 1}, \qquad g(u) = u + \kappa_R \ln(\rho_R e^{-u} + 1) + \kappa_C \ln(\rho_C e^{-u} + 1),$$

provided $\rho_C \neq \rho_R$. If $\rho_C = \rho_R = \rho$, then we use

$$g(u) = u + \alpha \ln(\rho e^{-u} + 1) - \frac{\beta}{\rho(\rho e^{-u} + 1)}.$$

We therefore, rescale the variable of integration $s = n\hat{s}/\omega$ in (39):

$$U\left(\frac{n\hat{t}}{\omega}\right) = \frac{I_0 n}{C_+ \omega} \int_0^{\hat{t}} \sin(n\hat{s}) f\left(\frac{n\hat{s}}{\omega\tau}\right) e^{\frac{\tau}{\theta_+}\left[g\left(\frac{n\hat{s}}{\omega\tau}\right) - g\left(\frac{n\hat{t}}{\omega\tau}\right)\right]} d\hat{s}$$

Hence, we obtain the formula we use in our Matlab code

$$Z(\omega) = \frac{in}{\pi C_+ \omega} \int_{2\pi}^{4\pi} e^{-in\hat{t}} \left(\int_0^{\hat{t}} \sin(n\hat{s}) f\left(\frac{n\hat{s}}{\omega\tau}\right) e^{\frac{\tau}{\theta_+}\left[g\left(\frac{n\hat{s}}{\omega\tau}\right) - g\left(\frac{n\hat{t}}{\omega\tau}\right)\right]} d\hat{s} \right) d\hat{t}. \tag{40}$$

In the frequency band where $n(\omega)/\omega \approx T_0$, we approximate, assuming that τ is large,

$$f\left(\frac{n\hat{s}}{\omega\tau}\right) \approx b_f + m_f \frac{n\hat{s}}{\omega\tau}, \qquad g\left(\frac{n\hat{s}}{\omega\tau}\right) \approx b_g + m_g \frac{n\hat{s}}{\omega\tau},$$

where the slopes m_f and m_g, and intercepts b_f and b_g are found from linear least squares fits of $f(x)$ and $g(x)$, $x \in [T_0/\tau, 2T_0/\tau]$. Then, all integrals in (40) can be computed explicitly. Up to exponentially small terms

$$Z(\omega) \approx \frac{b_f R_+}{m_g + i\omega\theta_+} + \frac{1}{2\omega\tau}\frac{m_f R_+}{m_g + i\omega\theta_+}\left(3T_0\omega + 3i - \frac{4im_g^2}{m_g^2 + \omega^2\theta_+^2}\right), \quad n(\omega) > 1,$$

where in the final expression we replaced $n(\omega)$ with $T_0\omega/(2\pi)$, which is valid exactly in the high frequency regime.

References

[1] P. Agarwal, M. E. Orazem, and L. H. Garcia-Rubio. Measurement models for electrochemical impedance spectroscopy: I. demonstration of applicability. *Journal of the Electrochemical Society*, 139(7):1917, 1992.

[2] P. Agarwal, M. E. Orazem, and L. H. Garcia-Rubio. Application of measurement models to impedance spectroscopy: III. Evaluation of consistency with the Kramers-Kronig relations. *Journal of the Electrochemical Society*, 142(12):4159, 1995.

[3] A. Bard and L. Faulkner. *Electrochemical Methods; Fundamentals and Applications*. Wiley Interscience, Hoboken, NJ, 2nd edition, 2000.

[4] E. Barsoukov and J. R. Macdonald, editors. *Impedance spectroscopy: theory, experiment, and applications*. John Wiley & Sons Inc., 2nd edition, 2005.

[5] B. A. Boukamp. A linear Kronig-Kramers transform test for immittance data validation. *Journal of the electrochemical society*, 142(6):1885, 1995.

[6] B. A. Boukamp. Distribution (function) of relaxation times, successor to complex nonlinear least squares analysis of electrochemical impedance spectroscopy? *Journal of Physics: Energy*, 2(4):042001, 2020.

[7] H. Brandstätter, I. Hanzu, and M. Wilkening. Myth and reality about the origin of inductive loops in impedance spectra of lithium-ion electrodes—a critical experimental approach. *Electrochimica acta*, 207:218–223, 2016.

[8] H.-M. Cho, Y. J. Park, and H.-C. Shin. Semiempirical analysis of time-dependent elementary polarizations in electrochemical cells. *Journal of The Electrochemical Society*, 157(1):A8–A18, 2009.

[9] C. Coelho, J. Phillips, and L. Silveira. Passive constrained rational approximation algorithm using nevanlinna-pick interpolation. In *Proceedings of the conference on Design, automation and test in Europe*, page 923. IEEE Computer Society, 2002.

[10] S. Cruz-Manzo and P. Greenwood. Low frequency inductive loop in eis measurements of an open-cathode polymer electrolyte fuel cell stack. impedance of water vapour diffusion in the cathode catalyst layer. *Journal of Electroanalytical Chemistry*, 900:115733, 2021.

[11] A. Dienstfrey and L. Greengard. Analytic continuation, singular-value expansions, and Kramers-Kronig analysis. *Inverse Problems*, 17(5):1307, 2001.

[12] J. S. Gnanaraj, R. W. Thompson, S. N. Iaconatti, J. F. DiCarlo, and K. M. Abraham. Formation and growth of surface films on graphitic anode materials for li-ion batteries. *Electrochemical and solid-state letters*, 8(2):A128–A132, 2005.

[13] Y. Grabovsky. Reconstructing Stieltjes functions from their approximate values: a search for a needle in a haystack. *SIAM J. Appl. Math.*, 82(4), 2022.

[14] Y. Grabovsky and N. Hovsepyan. On feasibility of extrapolation of the complex electromagnetic permittivity function using Kramers-Kronig relations. *SIAM J. Math Anal.*, 53(6):6993–7023, 2021.

[15] Y. Grabovsky and N. Hovsepyan. Optimal error estimates for analytic continuation in the upper half-plane. *Comm Pure Appl Math*, 2021. to appear.

[16] D. Klotz. Negative capacitance or inductive loop?–a general assessment of a common low frequency impedance feature. *Electrochemistry Communications*, 98:58–62, 2019.

[17] J. R. Partington et al. *Interpolation, identification, and sampling*. Number 17 in London Mathematical Society monographs (new series). Oxford University Press, 1997.

[18] A. Schiefer, M. Heinzmann, and A. Weber. Inductive low-frequency processes in pemfc-impedance spectra. *Fuel Cells*, 20(4):499–506, 2020.

[19] J. Scully, D. Silverman, and M. Kendig, editors. *Electrochemical Impedance: Analysis and Interpretation*. ASTM, 1993.

[20] A. Srivastava. Causality and passivity: From electromagnetism and network theory to metamaterials. *Mechanics of Materials*, 154:103710, 2021.

[21] S. Taibl, G. Fafilek, and J. Fleig. Impedance spectra of fe-doped srtio 3 thin films upon bias voltage: inductive loops as a trace of ion motion. *Nanoscale*, 8(29):13954–13966, 2016.

[22] M. Wohlers and E. Beltrami. Distribution theory as the basis of generalized passive-network analysis. *IEEE Transactions on Circuit Theory*, 12(2):164–170, 1965.

[23] Q.-C. Zhuang, X.-Y. Qiu, S.-D. Xu, Y.-H. Qiang, and S. Su. Diagnosis of electrochemical impedance spectroscopy in lithium-ion batteries. *Lithium Ion Batteries—New Developments*, 8:189–227, 2012.